

## **Implementing a power source to study the effect of power quality on the PEM water electrolyzer stack**

Lauri Järvinen, Vesa Ruuskanen, Joonas Koponen, Antti Kosonen, and Jero Ahola  
LUT UNIVERSITY  
P.O. BOX 20, 53851  
Lappeenranta, Finland  
Phone: +358 (50) 560-6293  
Email: lauri.jarvinen@lut.fi  
URL: <http://www.lut.fi>

Michael Hehemann  
FORSCHUNGSZENTRUM JÜLICH  
INSTITUT FÜR ENERGIE- UND KLIMAFORSCHUNG IEK-3  
Wilhelm-Johnen-Straße  
52428 Jülich, Germany  
Phone: +49 2461 61-5431  
URL: <http://www.fz-juelich.de/iek/iek-3>

### **Keywords**

«Power quality», «Electrolyzer», «Efficiency».

### **Abstract**

A power supply unit is implemented to experimentally study the effect of power quality on the water electrolyzer specific energy consumption. The power supply unit consists of a tailored signal generator and a laboratory DC power source used as an amplifier. The unit is capable of emulating the operation of thyristor bridge rectifiers.

### **Introduction**

Water electrolyzers may be the main electricity consumers in the future as the whole energy sector needs to be based on renewable energy sources [1]. Renewable hydrogen is needed to produce carbon neutral fuels for transportation and seasonal energy storage in the form of chemical energy, as well as to produce raw materials for the chemical industry [2, 3, 4, 5, 6].

According to Faraday's law of electrolysis, the hydrogen production rate of an electrolytic cell is linearly proportional to the applied current. Therefore, commercial electrolyzers apply relatively low voltage and high current. As an example of the DC voltage and current levels in MW-scale electrolyzers, the Power-to-Gas plant by ETOGAS in Werlte, Germany, was built up with three 2 MW alkaline water electrolyzers, whose nominal input voltage is 250 V and current 9000 A [7].

Owing to the requirement for high DC currents, the rectifiers in conventional industrial water electrolyzers are typically based on thyristors and diodes [8]. However, switching according to the line frequency generates harmonics to the supplied current and voltage causing additional heat losses in the water electrolysis process [9, 10]. The effect of current ripple on electrolytic cell lifetime is still a key research question for water electrolyzers [11, 12]. The effect of current ripple on the alkaline electrolytic cell is experimentally studied with theoretical current waveforms in [13]. It has been shown by simulations that the harmonics excited by the thyristor bridge have a significant effect on the performance of the alkaline

cell [14]. However, the experimental tests with thyristor bridge power supplies have not yet been reported in the literature for electrolytic cells in general.

In this paper, a power supply unit is implemented to enable electrolyzer cell testing under variable power quality. The unit is able to emulate thyristor bridge rectifier waveform characteristics in addition to the traditional DC, sine, and square waveforms. The unit consists of a myRIO (National Instruments) reconfigurable I/O device (used as a signal generator) and a laboratory DC power source (used as a power amplifier). Finally, the power supply unit is tested by supplying various waveforms to a proton exchange membrane (PEM) water electrolysis cell to enable further studies on the effects of power quality on electrolytic cells.

This paper is organized as follows. Section 2 introduces the power supply unit configuration and the thyristor waveform generation. In Section 3, the measured output waveforms of the unit are discussed both in the case of the dummy resistive load and the actual electrolyzer cell. Section 4 concludes the paper.

## Research methods

The designed power supply unit consists of three main parts: a myRIO embedded device, a signal amplifier, and a laboratory power source as shown in Fig. 1. MyRIO, which is a reconfigurable I/O device programmed with LabVIEW, is used as a signal generator. A laboratory DC power source is used as an amplifier for the generated signals. Several laboratory power sources were tested and the one with best frequency response was selected.

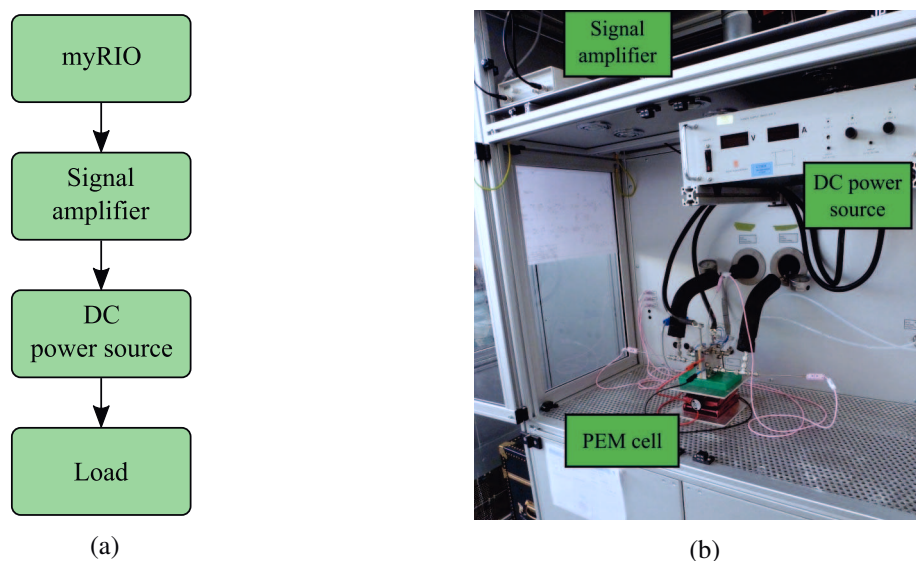


Fig. 1: (a) Key components of the power supply unit. MyRIO generates the control signal for the current waveform. The signal amplifier is used for control signal impedance matching. The DC power source acts as a power amplifier and generates the desired current output. In this study, both a dummy resistor and a PEM electrolyzer cell have been used as a load. (b) Experimental setup where a single PEM water electrolyzer cell is the load.

The current and voltage waveform measurement and acquisition system is the following: 0-Flucs-CT-600 0 A to 600 A current transducer (CAENels) with CT-BOX signal converter (CAENels) records the DC current, GN840B  $\pm 10$  V voltage sensor (HBM) records the DC voltage, and GEN2tB (HBM) is used for data logging.

In the previous studies, it has been shown that the electrolyzer stack or cell can be assumed to be a resistive load and their behavior can be described with a linear approximation [15]

$$U_{\text{cell}} = U_{\text{rev}} + Ri_{\text{cell}}A_{\text{cell}}, \quad (1)$$

where  $U_{\text{rev}}$  is the reversible voltage,  $R$  is the equivalent resistance,  $i_{\text{cell}}$  is the current density, and  $A_{\text{cell}}$  is the cell effective area. Therefore, the cell impedance can be emulated by just a resistor. This assumption is valid under in the linear region of the polarization curve of an electrolytic cell; at very low current densities the current-voltage relation is nonlinear as activation losses (reaction kinetics) have a relatively more significant role than ohmic losses [16]. A simulated polarization curve for a PEM water electrolysis cell is illustrated in Fig. 2.

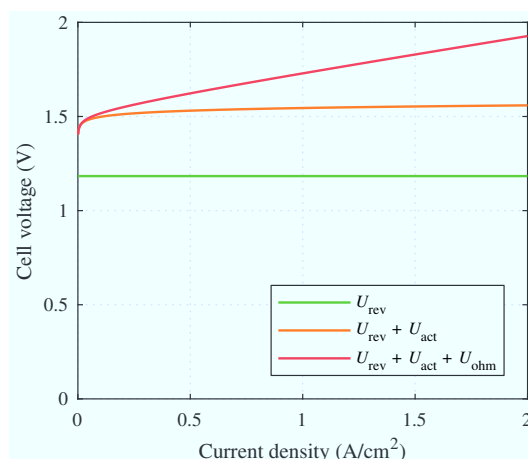


Fig. 2: Exemplary polarization curve of a PEM cell operating at 80 °C and balanced pressure of 1 bar. The total cell voltage is a sum of the reversible voltage  $U_{\text{rev}}$ , the activation overvoltage  $U_{\text{act}}$ , and the overvoltage due to ohmic losses in the cell elements  $U_{\text{ohm}}$ .

Another non-linear region may be observed at very high current densities if mass transport losses occur.

### Waveform generation

Signal waveforms are generated with LabVIEW. The standard DC, sine, and rectangular waveforms for the current control signal are generated with LabVIEW built-in functions. However, in the case of a grid frequency commutated thyristor bridge, the current waveform cannot be directly defined as the current is a function of load, grid voltage, and firing angle as shown for example in [14]. Therefore, the user needs to first select the grid voltage and frequency as well as the pulse number of the thyristor bridge per period, and the current mean value.

As the grid voltage is known, the firing angle producing the desired current mean value needs to be iterated. The voltage waveforms are calculated based on the selected firing angle. The period for each pulse is defined based on the pulse number of the bridge and the starting time is defined based on the firing angle. Based on the voltage waveform the current is calculated with a cell model (1) as shown in the Fig. 3. The current waveform mean value is compared with the user-defined value to select a new firing angle for the next iteration if necessary. Finally, the current waveform is scaled to be used as a current reference signal for the DC power source.

## Results

### Power source selection

Most laboratory DC power sources are designed to offer a high quality DC output with very limited dynamics. The passive filtering of the output limits the usable bandwidth if the DC power source is used as an amplifier. Therefore, multiple available power supplies were considered to select the suitable one. First criterion was the capability to output a DC current of 100 A for an electrolytic cell. Two available power sources meeting the first criterion were selected for further testing.

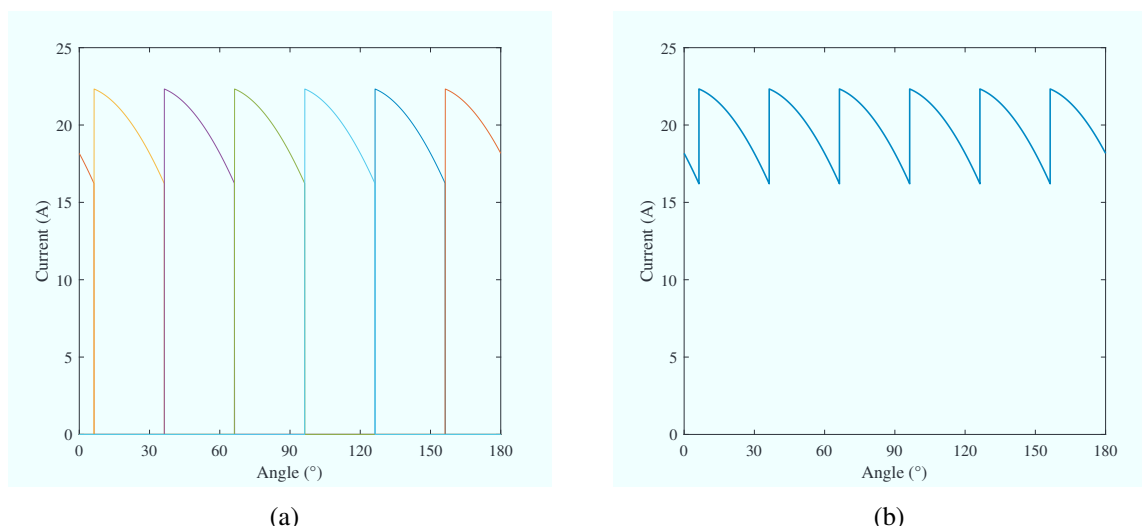


Fig. 3: Forming the current waveform of the 12-pulse thyristor bridge in the LabVIEW environment. (a) Individual pulses of the bridge with different colors. (b) Full output waveform is achieved by repeating the single pulse currents.

Comparison between two power sources, Sorensen SGA 100-150 and Delta Elektronika SM 30-100 D, showed that the Delta Elektronika power supply is able to produce an acceptable square waveform even at 600 Hz frequency—the dominating harmonic in the case of the 12-pulse thyristor bridge with 50 Hz grid frequency. Meanwhile, the Sorensen power supply failed to output an acceptable square waveform at  $\geq 50$  Hz. Therefore, Delta Elektronika was selected to be used as an amplifier.

### Output waveforms

Finally, all the desired current waveforms were tested by supplying a 50 mΩ resistor—an electrical resistance in the range of the total impedance of the electrolyzer stack. The key waveforms are shown in Fig. 4.

It can be stated that the power supply unit is able to generate the desired current and voltage waveforms up to frequency of 600 Hz without significant deformations.

### Tests with a PEM electrolysis cell

In a test rig at Forschungszentrum Jülich, a PEM water electrolysis cell with an active area of 17.64 cm<sup>2</sup> was supplied with sine waveforms under variation of the DC offset. Further, a similar cell was supplied with 6- and 12-pulse thyristor bridge waveforms, which are typical for industrial water electrolyzers. Generated test sine waveforms supplied to the PEM water electrolysis cell are illustrated in Fig. 5.

The 6-pulse thyristor bridge waveforms at DC current set point 10 A as well as the discrete Fourier transforms (DFT)—which presents the amplitudes of each constituent frequency component in the frequency domain—for the current and voltage are presented in Fig. 6. In the case of the 6-pulse thyristor bridge, the resulting root mean square (RMS) value of cell DC voltage is 0.3% higher than the mean value of voltage. For cell current, the resulting RMS value is 32% higher than the mean value of current. In Fig. 6d, the harmonic amplitudes show the notable 300 Hz AC component—and its multiples—typical for industrial 6-pulse thyristor rectifiers. Now the 300 Hz component has a higher amplitude than the DC component, which indicates that even relatively small variations in voltage produce great variations in the current supplied to PEM water electrolysis cells.

The 12-pulse thyristor bridge waveforms at DC current set point 10 A as well as the DFTs for the current and voltage are presented in Fig. 7. In the case of the 12-pulse thyristor bridge, the resulting RMS value of cell DC voltage is 0.09% higher than the mean value of voltage. For cell current, the resulting RMS value is 11% higher than the mean value of current. In Fig. 7d, the harmonic amplitudes show the desired 600 Hz AC component—and its multiples—typical for industrial 12-pulse thyristor rectifiers.

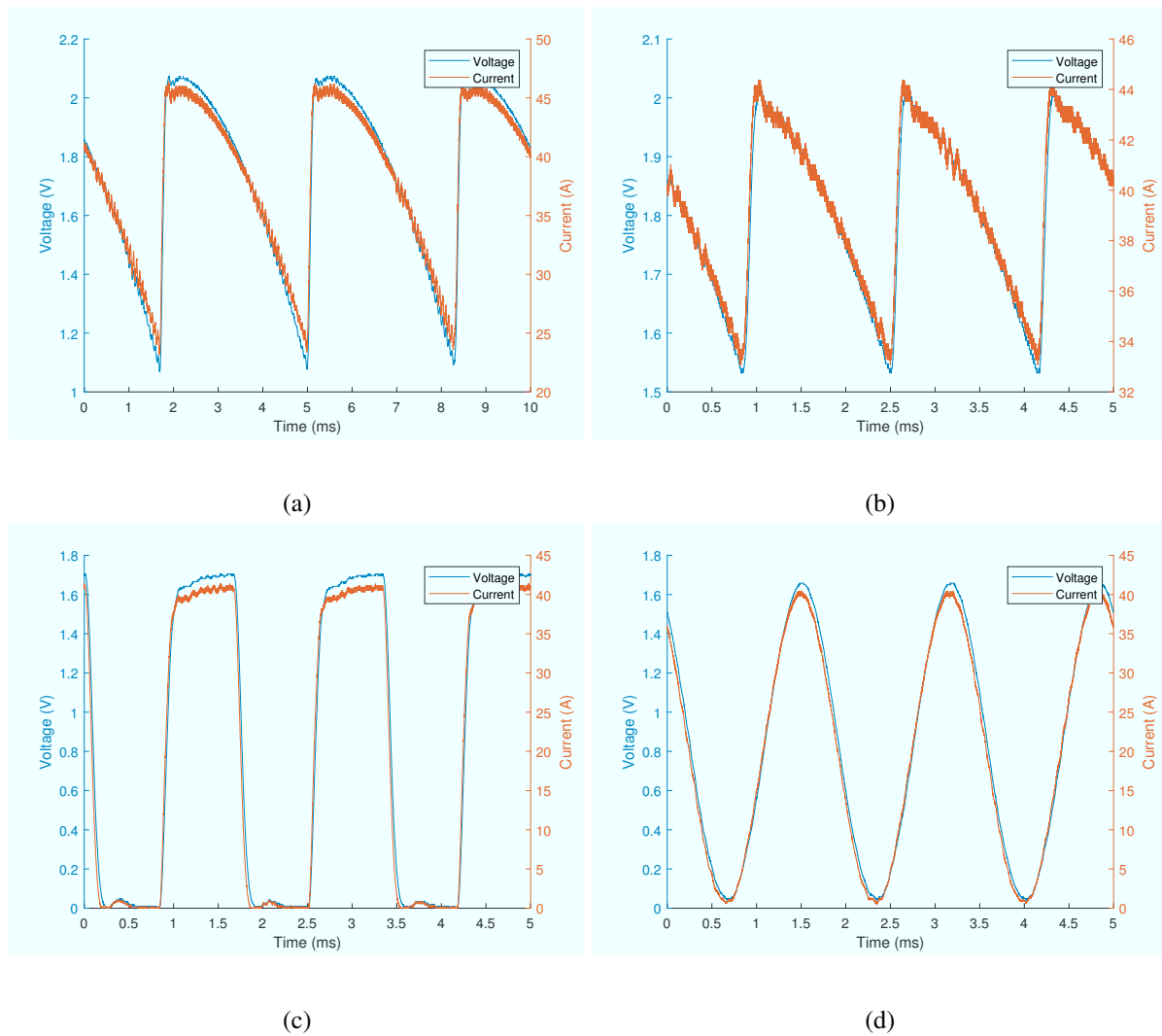


Fig. 4: Example output current and voltage waveforms of the power source. (a) Thyristor 300 Hz, phase angle 30°. (b) Thyristor 600 Hz, phase angle 30°. (c) Square wave 600 Hz. (d) Sine wave 600 Hz.

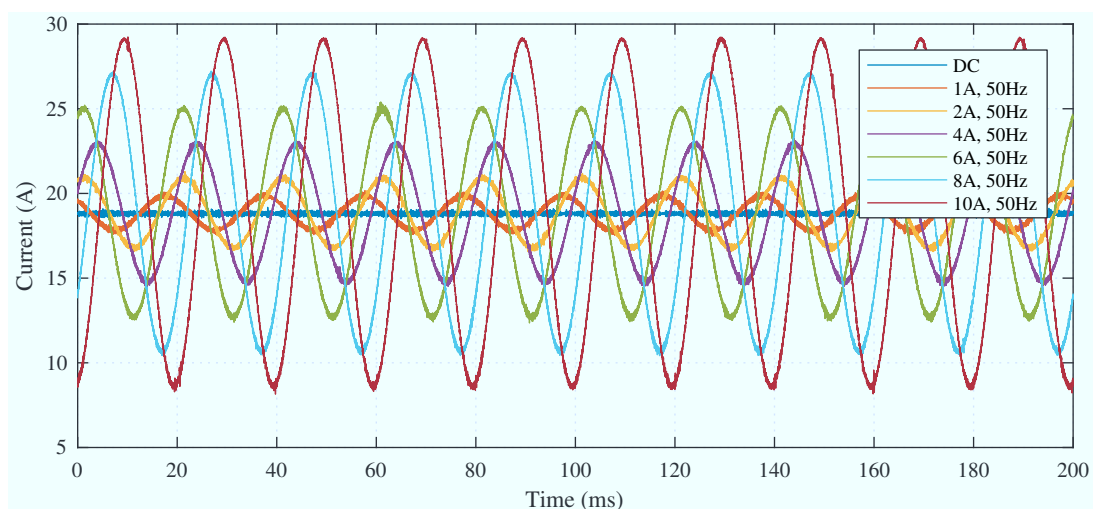


Fig. 5: Measured current waveforms supplied to a PEM water electrolysis cell. The DC current density is 1 A/cm<sup>2</sup> and the AC ripple amplitude is varied.

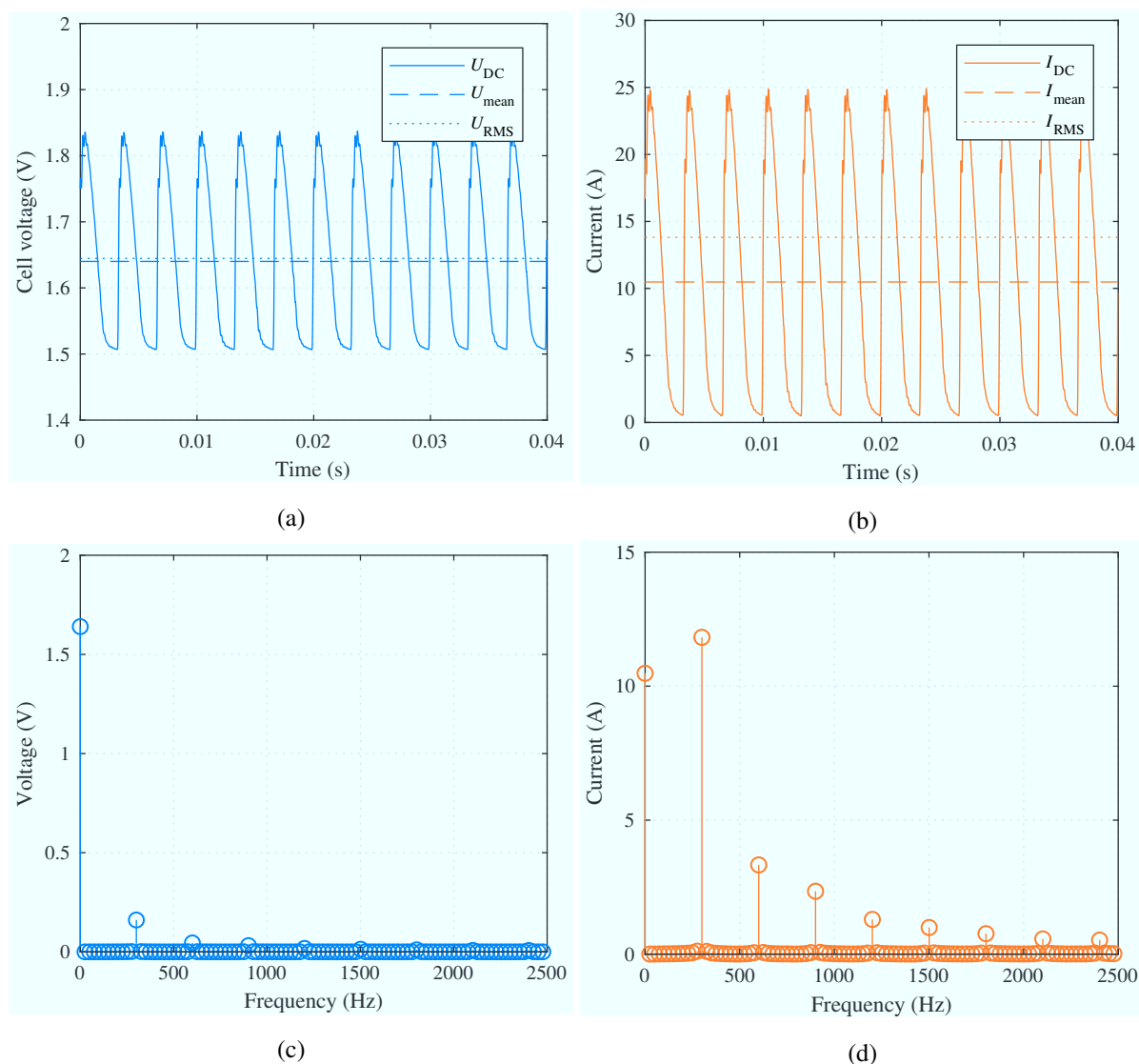


Fig. 6: Measured current and voltage waveforms supplied to a PEM water electrolyzer cell, when the DC current set point is 10 A with a 6-pulse thyristor bridge. (a) Voltage waveform. (b) Current waveform. (c) DFT of the voltage time-series data. (d) DFT of the current time-series data.

It can be seen that the power supply unit is able to generate the desired current waveforms as the load is the actual electrolyzer cell as well as in the case of the dummy load studied above.

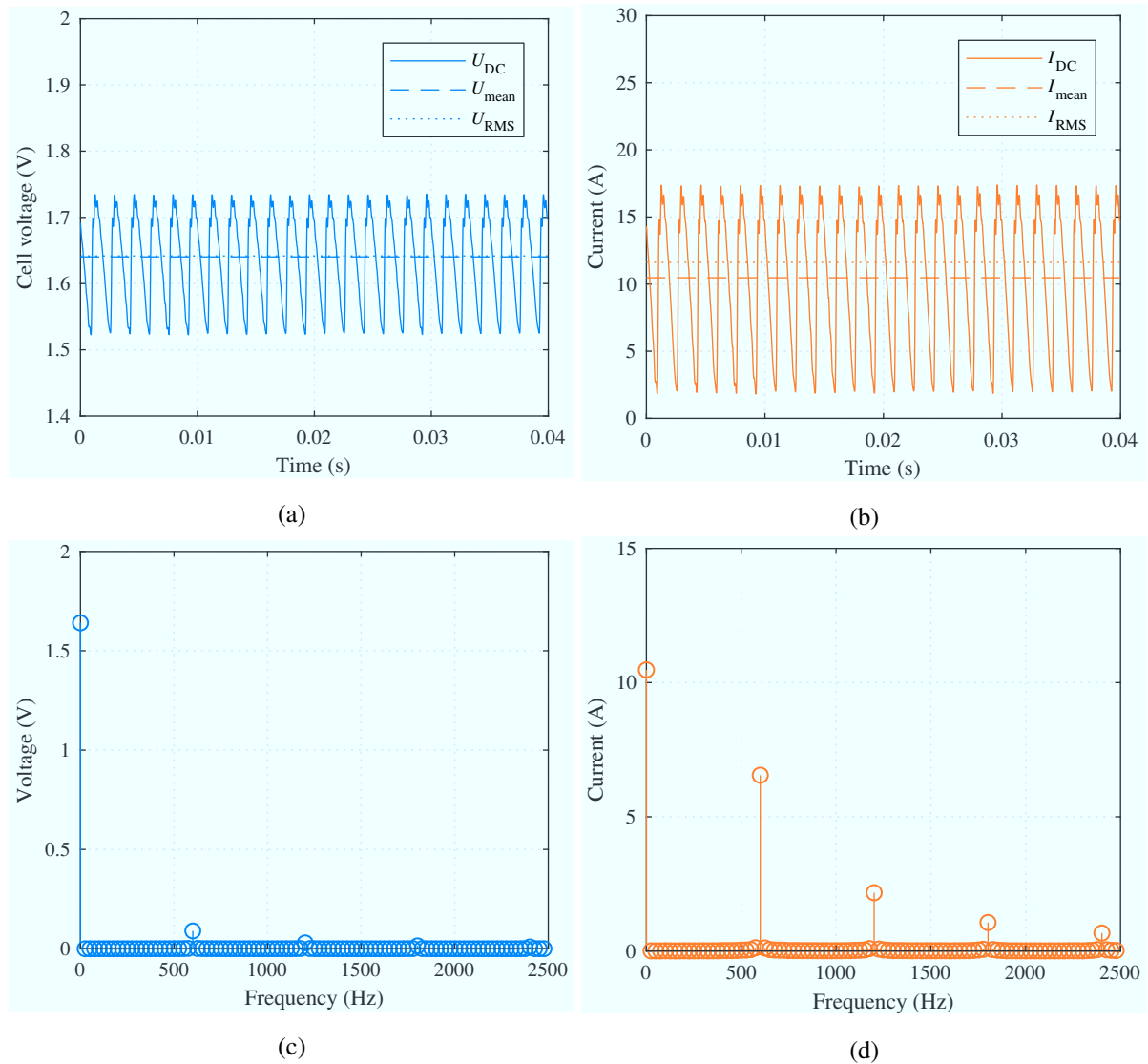


Fig. 7: Measured current and voltage waveforms supplied to a PEM water electrolyzer cell, when the DC current set point is 10 A with a 12-pulse thyristor bridge. (a) Voltage waveform. (b) Current waveform. (c) DFT of the voltage time-series data. (d) DFT of the current time-series data.

## Conclusions

In this work, a power supply unit for electrolyzer cell testing was implemented. A laboratory DC power supply was used as an amplifier and myRIO was used as a tailored signal generator. The system was tested to be able to generate current and voltage waveforms of the 6- and 12-pulse thyristor bridge rectifiers in addition to traditional sine, rectangular and DC waveforms. The implemented power supply will be used in future work to study the effect of power quality on PEM water electrolysis cells in terms of specific energy consumption and degradation rate. Long-term testing will be carried out with and without current ripple exposure at different cell membrane thicknesses.

## References

- [1] P. Schmidt, W. Zittel, W. Weindorf, and T. Raksha, "Renewables in Transport 2050 Empowering a sustainable mobility future with zero Final Report," FVV, Tech. Rep., 2016. [Online]. Available: [http://www.lbst.de/news/2016\\_docs/FVV\\_H1086\\_Renewables-in-Transport-2050-Kraftstoffstudie\\_II.pdf](http://www.lbst.de/news/2016_docs/FVV_H1086_Renewables-in-Transport-2050-Kraftstoffstudie_II.pdf)
- [2] M. Fasihi, D. Bogdanov, and C. Breyer, "Techno-economic assessment of Power-to-Liquids (PtL) fuels production and global trading based on hybrid PV-wind power plants," in *Proc. 10th Int. Renewable Energy Storage Conf. (IRES '16)*, Düsseldorf, Germany, Mar. 2016.
- [3] G. Pleßmann, M. Erdmann, M. Hlusiak, and C. Breyer, "Global energy storage demand for a 100% renewable electricity supply," *Energy Procedia*, vol. 46, pp. 22–31, 2014.
- [4] J. Koponen, A. Kosonen, K. Huoman, J. Ahola, T. Ahonen, and V. Ruuskanen, "Specific energy consumption of PEM water electrolyzers in atmospheric and pressurised conditions," in *Proc. 18th European Conf. on Power Electron. and Applicat. (EPE '16-ECCE Europe)*, Karlsruhe, Germany, Sep. 2016.
- [5] A. Kosonen, J. Koponen, K. Huoman, J. Ahola, V. Ruuskanen, T. Ahonen, and T. Graf, "Optimization strategies of PEM electrolyser as part of solar PV system," in *Proc. 18th European Conf. on Power Electron. and Applicat. (EPE '16-ECCE Europe)*, Karlsruhe, Germany, Sep. 2016.
- [6] J. Koponen, A. Kosonen, V. Ruuskanen, K. Huoman, M. Niemelä, and J. Ahola, "Control and energy efficiency of PEM water electrolyzers in renewable energy systems," *Int. J. of Hydrogen Energy*, vol. 42, no. 50, pp. 29 648–29 660, Dec. 2017.
- [7] Erdgas. [Accessed: 21-Dec-2017]. [Online]. Available: [https://www.di-verlag.de/media/content/gwf-GE/gwf\\_Gas\\_9\\_13/gwf-GE\\_09\\_2013\\_fb\\_Rieke.pdf?xaf26a=7607be2af411325a0ddff83247813f87](https://www.di-verlag.de/media/content/gwf-GE/gwf_Gas_9_13/gwf-GE_09_2013_fb_Rieke.pdf?xaf26a=7607be2af411325a0ddff83247813f87).
- [8] A. Ursúa, P. Sanchis, and L. Marroyo, "Chapter 14 - electric conditioning and efficiency of hydrogen production systems and their integration with renewable energies," in *Renewable Hydrogen Technologies*, L. Gandía, G. Arzamendi, and P. Diéguez, Eds. Amsterdam: Elsevier, 2013, pp. 333–360.
- [9] A. Ursúa, L. Marroyo, E. Gubía, L. M. Gandía, P. M. Diéguez, and P. Sanchis, "Influence of the power supply on the energy efficiency of an alkaline water electrolyser," *Int. J. Hydrogen Energy*, vol. 34, no. 8, pp. 3221–3233, May. 2009.
- [10] A. Ursúa, I. S. Martín, and P. Sanchis, "Design of a programmable power supply to study the performance of an alkaline electrolyser under different operating conditions," in *2nd IEEE Int. Energy Conf. and Exhibition (ENERGYCON '12)*, Florence, Italy, Sep. 2012, pp. 259–264.
- [11] L. Bertuccioli, A. Chan, D. Hart, F. Lehner, B. Madden, and E. Standen, *Study on development of water electrolysis in the EU*. Final report in fuel cells and hydrogen joint undertaking, Feb. 2014.
- [12] C. Rakousky, U. Reimer, K. Wippermann, S. Kuhri, M. Carmo, W. Lueke, and D. Stolten, "Polymer electrolyte membrane water electrolysis: Restraining degradation in the presence of fluctuating power," *J. Power Sources*, vol. 342, pp. 38–47, 2017.
- [13] Z. Dobó and Á. B. Palotás, "Impact of the current fluctuation on the efficiency of Alkaline Water Electrolysis," *Int. J. Hydrogen Energy*, vol. 42, no. 9, pp. 5649–5656, 2017.
- [14] J. Koponen, V. Ruuskanen, A. Kosonen, M. Niemelä, and J. Ahola, "Effect of converter topology on the specific energy consumption of alkaline water electrolyzers," *IEEE Trans. Power Electron.*, vol. 34, no. 7, pp. 6171–6182, Jul. 2019.
- [15] J. Koponen, V. Ruuskanen, A. Kosonen, M. Niemelä, and J. Ahola, "Considering power quality in energy efficiency of alkaline water electrolyzers," in *Proc. 20th European Conf. on Power Electron. and Applicat. (EPE '18-ECCE Europe)*, Riga, Latvia, Sep. 2018.
- [16] M. Schalenbach, G. Tjarks, M. Carmo, W. Lueke, M. Mueller, and D. Stolten, "Acidic or alkaline? towards a new perspective on the efficiency of water electrolysis," *J. Electrochem. Soc.*, vol. 163, no. 11, pp. F3197–F3208, 2016.